CHAPTER 5

TINOSPORA CORDIFOLIA EXTRACT: NATURAL CORROSION INHIBITOR FOR MILD STEEL IN ACID MEDIA

This chapter introduces *Tinospora cordifolia* extract's (TCE) inhibiting capacity on mild steel in 1 M HCl and 0.5 M H_2SO_4 by weight loss techniques, electrochemical and surface morphological studies. Effects of temperature, concentration of TCE and acid medium on inhibition efficiency are evaluated employing statistical tools such as response surface methodology (RSM) and Box-Behnken design (BBD). The research world has revealed medicinal characteristics of *Tinospora cordifolia* leaves, but their corrosion resistance properties with various competencies are not yet investigated. *Tinospora cordifolia* belongs to the Menispermaceae family, comprised of so many phytochemicals. Tinosponone is the major metabolite in *Tinospora cordifolia* leaf extract, which is a sesquiterpene[163]. Its structure is shown in Fig. 5.1. Berberine, tembetarine, tinocordioside, syringin, magnoflorine and 20-hydroxyecdysone are some of the minor chemical compounds in it.

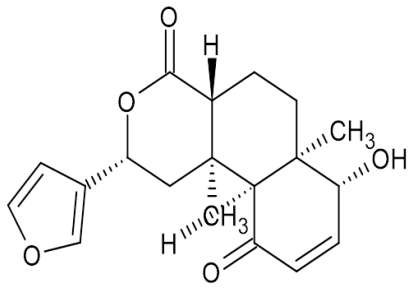

Fig. 5.1: Structure of tinosponone

Tinospora cordifolia

Results and discussions

Phytochemical screening of TCE

The presence of major phytochemicals in TCE was confirmed using different tests, and the results are given in Table 5.1.

Table 5.1: Phytochemical screening of TCE

Sl. No.	Compounds	Tests	Results
1	Alkaloids	Mayers reagent	−−
2	Steroids	Salkowaski's test	++
3	Phenolic compounds	Potassium ferrocyanide test	++
4	Flavanoids	Sodium hydroxide test	++
5	Saponins	Froth test	++
6	Tannins	Lead acetate test	++
7	Cardiac glycosides	Conc. sulphuric acid test	++
8	Coumarin	Alcoholic NaOH test	++
9	Quinones	Conc. sulphuric acid test	++

++ (present), − − (Absent)

FTIR spectroscopy

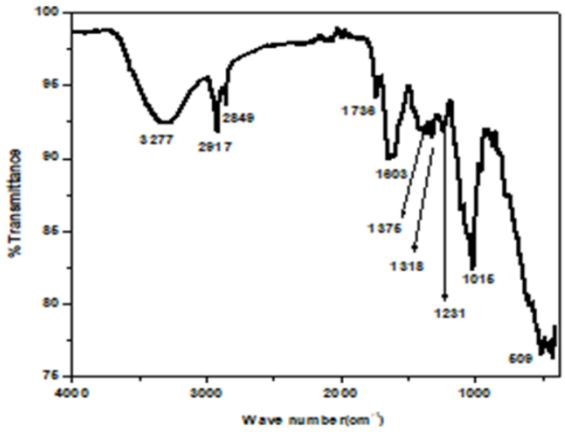

Fig. 5.2: FTIR spectrum of TCE

The FTIR spectrum of TCE revealed characteristic stretching and bending frequencies for various bonds, drawn in Fig. 5.2. Broadband at 3277 cm^{-1} denotes O-H stretching. Two sharp bands at 2917 cm^{-1} and 2849 cm^{-1} represents alkyl C-H stretching vibrations. >C=O stretching vibration appears at 1736 cm^{-1}. This peak can be assigned to six-membered cyclic lactones. The bands at 1603 cm^{-1} and 1318 cm^{-1} can be accredited to >C=C stretching vibrations. C-O bending pulse appears as a weak band at 1231 cm^{-1} and 1016 cm^{-1}. This peak can be ascribed to characteristic peaks for the furan ring. In summary, distinct peaks of TCE can be attributed to heteroatoms, aromatic rings, and unsaturated compounds.

Weight loss measurements

❖ ***Effect of concentration***

Corrosion inhibition efficiency (ηℵ) and corrosion rate (υ) found by weight loss technique on mild steel in 1 M HCl and 0.5 M H_2SO_4 with varying concentrations (0-5 v/v %) of TCE have been calculated. (Table 5.2)

Table 5.2: Weight loss measurements of mild steel with and without TCE in 1 M HCl and 0.5 M H_2SO_4 at room temperature for 24 hrs

Conc. (v/v %)	Corrosion rate (mm/yr)		Inhibition efficiency (ηℵ)	
	1 M HCl	0.5 M H_2SO_4	1 M HCl	0.5 M H_2SO_4
Blank	3.9500	35.570	-	-
1	0.7852	17.763	80.12	50.06
2	0.5731	13.370	85.49	62.41
3	0.4530	9.038	88.53	74.59
4	0.3365	7.533	91.48	78.82
5	0.2081	6.214	94.73	82.53

An augment in inhibition power was noticed from the data by raising TCE concentration in both acid media. Also seen that TCE behaves as an efficient green corrosion inhibitor in 1 M HCl, attaining maximum inhibition efficacy of 94.73% and 82.53% in 0.5 M H_2SO_4 at 5% TCE concentration. In HCl solution, TCE exhibit more inhibition capacity compared to H_2SO_4 solution. It may be due to the effective adsorption of Cl^- ions on the metal surface than SO_4^{2-} ions since halide ions are more electronegative. It may lead to more adsorption of cationic organic molecules on the metal surface to inhibit metal dissolution. At the same time, SO_4^{2-} ions were adsorbed on the metal surface poorly. It causes lesser surface coverage on metal. So, the fraction of TCE molecules adsorbed on mild steel surface is low, and hence, metal suffers a high corrosion rate in the H_2SO_4 medium.

❖ ***Effect of temperature***

Stability of the protective film of TCE by adsorption on mild steel surface was described by performing temperature studies[63]. Here, the impact of temperature on the corrosion control was accomplished by weight loss measurements in 1 M HCl and 0.5 M H_2SO_4 with varying TCE concentrations at different temperatures (303-333 K) for 24 hrs. Inhibition potential was calculated and given in Table 5.3 and graphically depicted in Fig. 5.3. It showed that the rate of corrosion rises with an enhancement in temperature for a fixed concentration. When the temperature raised from 303 K to 333 K, efficiency lowered from 94.73% to 62.64% for 5% TCE concentration in HCl medium. A similar observation can see in the H_2SO_4 medium, where the inhibition efficiency decreased from 82.53% to 66.61% for the same strength and temperature range. This trend may be ascribed to the metal surface changes such as instant engraving, crack, detachment of adsorbed film, decay, or reordering of the inhibitor when the temperature rises in both acids and thereby decreases inhibition potency. So, discrepancies in temperature influenced the metal disintegration, action of inhibitor either adsorption or desorption and corrosion control.

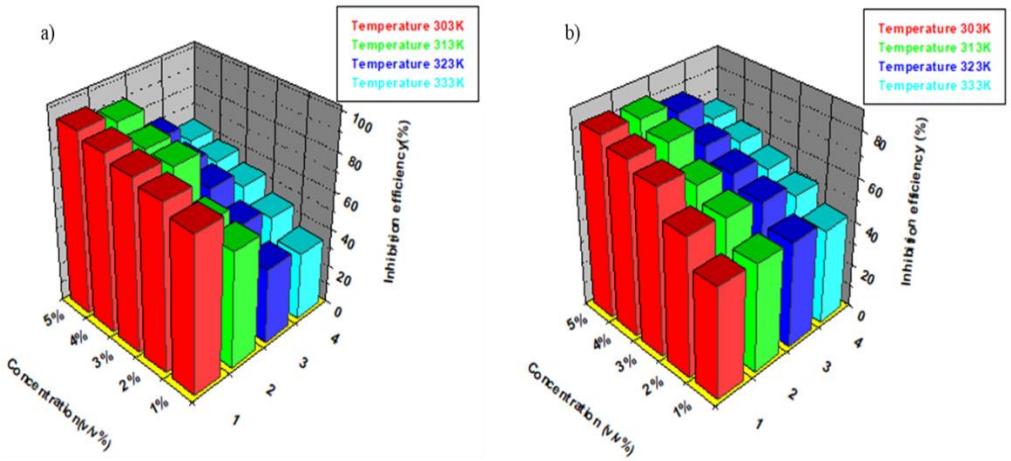

Fig. 5.3: Variation in inhibition efficiency of TCE in a) 1 M HCl b) 0.5 M H_2SO_4 at elevated temperatures

Table 5.3: Corrosion rate (υ) and inhibition efficiency (η%) of TCE in 1 M HCl and 0.5 M H_2SO_4 at different temperatures for 24 hrs

Medium	Conc. (v/v%)	υ (303K)	η% (303K)	υ (313K)	η% (313K)	υ (323K)	η % (323K)	υ (333K)	η% (333K)
1 M HCl	Blank	3.95	-	13.11		22.05	-	31.77	-
	1	0.78	80.12	5.23	60.11	13.54	38.61	20.48	35.54
	2	0.57	85.49	4.72	64.00	10.69	51.53	17.36	45.36
	3	0.45	88.53	2.15	83.60	8.23	62.68	14.69	53.76
	4	0.33	91.48	2.07	84.21	7.45	66.22	12.98	59.14
	5	0.20	94.73	1.26	90.39	6.15	72.11	11.87	62.64
0.5 M H_2SO_4	Blank	35.57	-	58.27	-	86.25	-	106.2	-
	1	17.76	50.06	29.69	49.04	44.95	47.88	60.04	43.49
	2	13.37	62.41	23.08	60.39	36.58	57.58	51.64	51.40
	3	9.03	74.59	19.36	66.77	31.95	62.95	45.91	56.79
	4	7.53	78.82	12.88	77.89	27.23	68.42	40.12	62.24
	5	6.21	82.53	10.77	81.51	20.14	76.64	35.48	66.61

Arrhenius equation was used to plot log K vs 1/T curves for metal corrosion in the presence and absence of TCE in acid media. Fig. 5.4 a) and Fig. 5.5 a) show Arrhenius plots. Slopes of the straight lines were fit to evaluate the activation energy of corrosion in acid media. Transition state theory renders the calculation of thermodynamic parameters such as enthalpy of activation (ΔH^*) and entropy of activation (ΔS^*). Linear plots of log K/T vs 1/T for the mild steel corrosion with and without TCE are shown in Fig. 5.4 b) and Fig. 5.5 b). All the thermodynamic parameters and activation energy derived from these plots were tabulated in Table 5.4, which established that the activation energy of corrosion increases with an increase in TCE concentration due to the growing energy barrier. It also emphasized an activated complex compound formed by the interaction between the inhibitor and mild steel[164]. Positive value of enthalpy described the endothermic character of the metal corrosion process[165]. ΔS^* values were also increased by adding TCE concentration. Negative values of the entropy of activation for corrosion in the absence of TCE mentioned a decrease in randomness for the activated complex compared to the reactants. Disorderliness of the activated complex increases as the concentration of TCE raises and ΔS^* possessed

positive values. In the case of H_2SO_4 medium, ΔS^* value in the absence of TCE was seen to be largely negative compared to other ΔS^* values in the presence of TCE, and it became less negative as concentration increases.

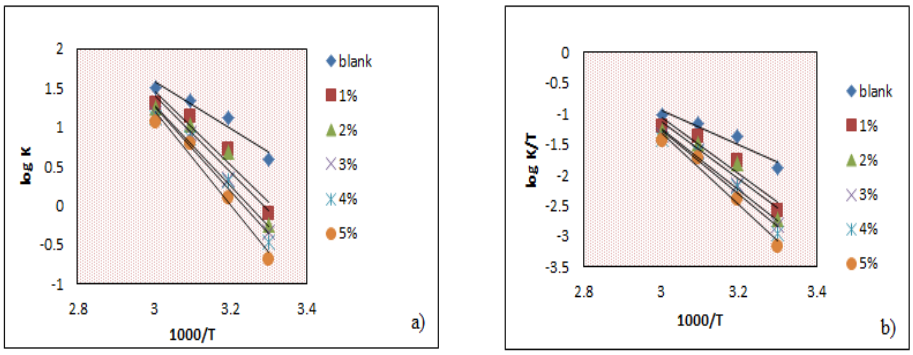

Fig. 5.4: Arrhenius plots of a) log K vs 1000/T b) log K/T vs 1000/T with and without TCE in 1 M HCl

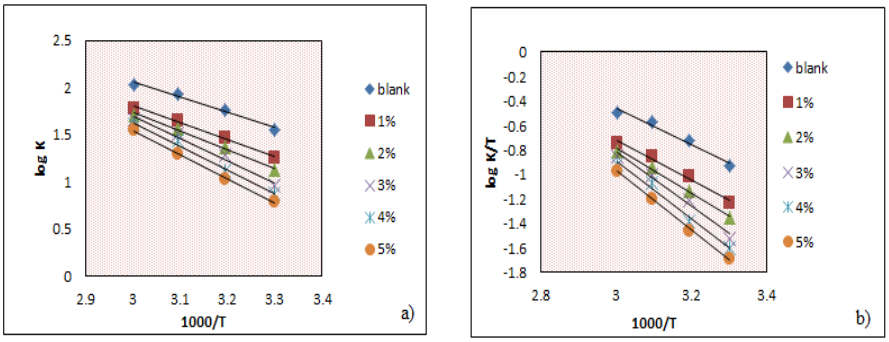

Fig. 5.5: Arrhenius plots of a) log K vs 1000/T b) log K/T vs 1000/T with and without TCE in 0.5 M H_2SO_4

Table 5.4: Thermodynamic parameters of mild steel corrosion with and without TCE in 1 M HCl and 0.5 M H_2SO_4

Medium	Conc. (v/v %)	E_a (kJ mol^{-1})	A	ΔH^* (kJ mol^{-1})	ΔS^* (J $mol^{-1}K^{-1}$)
1 M HCl	Blank	57.24	3.58×10^{10}	54.60	-44.78
	1	90.79	4.95×10^{15}	88.15	53.66
	2	93.51	1.13×10^{16}	90.87	60.51
	3	99.28	6.98×10^{16}	96.64	75.66
	4	103.28	2.76×10^{17}	100.64	87.09
	5	115.60	2.14×10^{19}	112.97	123.27
0.5 M H_2SO_4	Blank	30.96	8.16×10^{6}	28.30	-114.51
	1	34.23	1.47×10^{7}	31.59	-109.62
	2	37.95	4.82×10^{7}	35.31	-99.74
	3	45.29	6.31×10^{8}	42.65	-78.34
	4	48.42	1.66×10^{9}	45.78	-70.33
	5	49.06	1.73×10^{9}	46.42	-69.97

Adsorption isotherms

Adsorption isotherm studies provide interaction mechanism between inhibitor molecules and mild steel. Among different adsorption isotherm models such as Langmuir, El-Awady, Frumkin, Temkin, Freundlich, Flory-Huggins isotherms, the best adsorption isotherm model of TCE in 1 M HCl and 0.5 M H_2SO_4 was explored by fitting the extent of surface coverage (θ) and corrosion rate into it. Langmuir adsorption isotherm was found to be the best model with R^2 values of 0.9987 and 0.9974 in 1 M HCl and 0.5 M H_2SO_4, respectively. Fig. 5.6 represents Langmuir adsorption isotherms of TCE on mild steel in 1 M HCl and 0.5 M H_2SO_4 at room temperature.

Mechanism of adsorption can be estimated from the values of ΔG^0_{ads} which is related to adsorption equilibrium constant K_{ads}. In the present work, ΔG^0_{ads} for TCE-mild steel adsorptions were -30.37 and -27.15 kJ mol^{-1} in 1 M HCl and 0.5 M H_2SO_4, respectively, which showed the nature of adsorption of TCE molecules on mild steel surface as both physisorption and chemisorption[166]. K_{ads} values for TCE adsorption were calculated as 3362.475 and 931.185 in 1 M HCl and 0.5 M H_2SO_4, respectively. The higher inhibition potency of TCE in HCl than H_2SO_4 medium can be justified by evaluating the values of $K_{ads,}$ which was more significant for HCl than H_2SO_4.

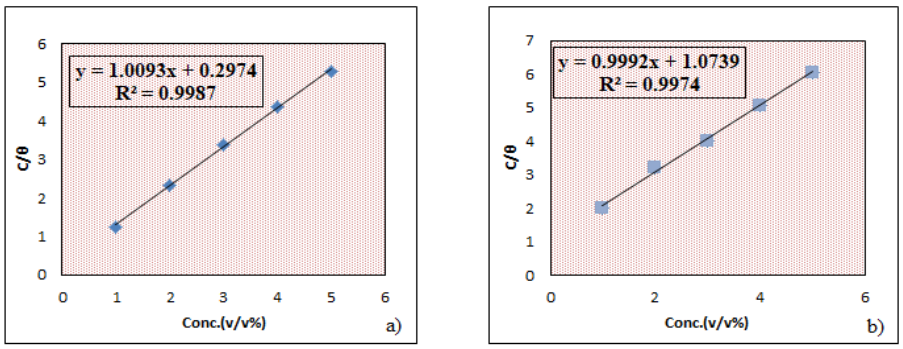

Fig. 5.6: Langmuir adsorption isotherm of TCE on mild steel in a) 1 M HCl and b) 0.5 M H_2SO_4

Fig. 5.7 portrays the possible surface behaviour of TCE molecules on mild steel. Even though TCE contains various components, the principal component is regarded as an authoritative compound for corrosion inhibition. The effective adsorption of tinosponone molecules by donating electrons from oxygen atoms in the furan ring, –OH, lactone functional groups, and π-electrons in the aromatic system causes the formation of a protective film on the metal surface and thereby mitigates metal corrosion. Moreover, tinosponone molecules may interact via back donation of 'd' electrons from the metal to π^* orbitals of tinosponone molecules. Besides this interaction, physisorption of TCE molecules was involved. Initially, chloride/sulfate ions present in the acid solution approach on the surface of mild steel and continue as a cathode. The cationic molecules of TCE, which are considerably larger than acid ions, were adsorbed on the metal surface by the substitutional adsorption process in the anodic and cathodic process of metal corrosion and decreased metal dissolution rate.

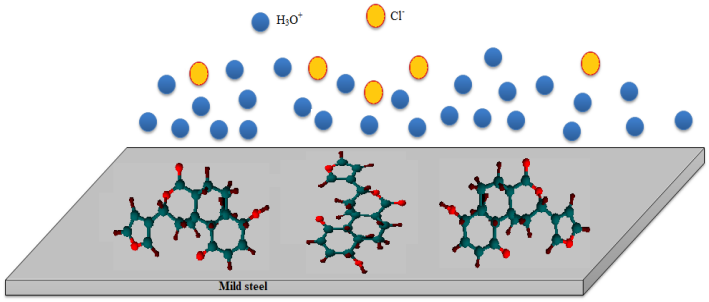

Fig. 5.7: Interaction diagram between tinosponone molecules and mild steel surface in acid media

Electrochemical impedance spectroscopy

The corrosion response of mild steel in 1 M HCl and 0.5 M H_2SO_4 solutions with various concentrations of TCE (0-5 v/v %) were demonstrated using EIS at 30^0C. In the present investigation, Randle's circuit (Fig. 1.8) was adjudged as an equivalent circuit. Fig. 5.8 and Fig. 5.9 shows Nyquist plots and Bode plots. Nyquist plots are not in an absolute semicircular shape. It can be interpreted as the result of surface inhomogeneity.

The adsorption phenomenon on the surface or development of porous or non-porous passivation layer on coating is the root cause for surface in-homogeneity[167]. Nyquist plots evinced a single capacitive loop for each concentration. It may be due to the occurrence of a charge transfer reaction at the electrode/solution interface. On examining the plots, it can be seen that the diameter of the semicircle increases by the addition of TCE concentration.

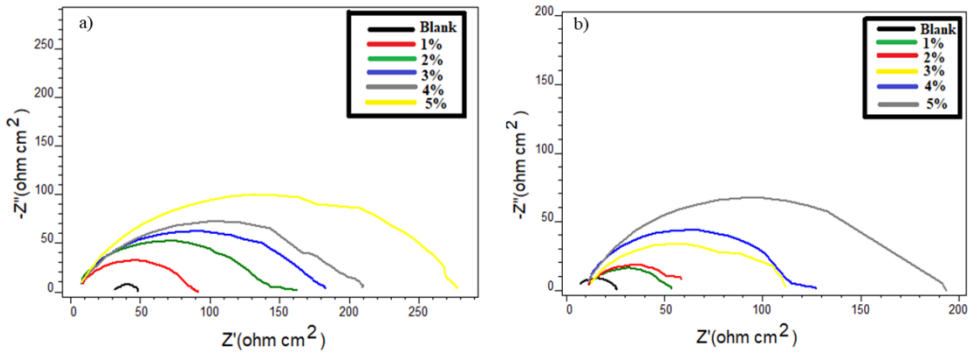

Fig. 5.8: Nyquist plots of mild steel with and without TCE in a) 1 M HCl and b) 0.5 M H_2SO_4

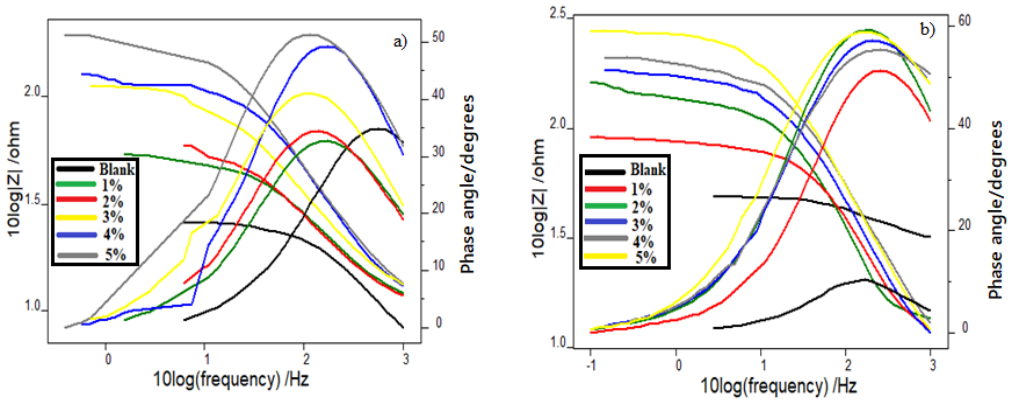

Fig. 5.9: Bode plots of mild steel with and without TCE in a) 1 M HCl and b) 0.5 M H_2SO_4

Table 5.5 clearly showed that R_{ct} values are directly proportional to TCE concentration, indicating that the mild steel corrosion is mitigated by the inhibitor TCE. Conversely, C_{dl} values decreased by the addition of TCE. This is due to a drop in the dielectric constant or a rise in the thickness of the electrical double layer. It recommends the formation of an interfacial protective layer between metal and acid[168]. Inhibition

efficiency of TCE attained 93.51% in 1 M HCl and 88.68% in 0.5 M H_2SO_4 for the highest concentration under supervision.

Table 5.5: Impedance parameters of mild steel in 1 M HCl and 0.5 M H_2SO_4 with and without TCE

Conc. (v/v %)	1 M HCl			0.5 M H_2SO_4		
	R_{ct} (Ωcm^2)	C_{dl} (μFcm^{-2})	η_{EIS}%	R_{ct} (Ωcm^2)	C_{dl} (μFcm^{-2})	η_{EIS}%
Blank	15.7	78.75	-	18.1	47.39	-
1	74.5	62.8	78.92	37.3	46.5	51.47
2	125	48.9	87.44	41.3	44.1	56.17
3	153	47.5	89.73	86.3	39.0	79.02
4	174	45.6	90.97	100	40.3	81.9
5	242	42.1	93.51	160	32.6	88.68

Potentiodynamic polarization studies

Potentiodynamic polarization studies on mild steel were carried out to evaluate the protective ability of TCE on the surface of mild steel in 1 M HCl and 0.5 M H_2SO_4. Fig. 5.10 and Fig. 5.11 exhibit Tafel and linear polarisation plots, and Table 5.6 reveal polarization parameters such as corrosion current densities (i_{corr}), corrosion potential (E_{corr}), cathodic Tafel slope (b_c), anodic Tafel slope (b_a) and polarization resistance (R_p). On close observation to the Table as mentioned above, it is clear that there was a remarkable decrease in i_{corr} values when TCE concentration increased. It can be pointed out that there is strong resistance in the corrosion process[55]. So, inhibition efficacy was found to be supplemented with an increase in concentration. The higher inhibition power on mild steel surface was displayed by 5% TCE concentration in HCl and H_2SO_4 media as 94.22% and 75%, respectively. A lower efficiency in H_2SO_4 than HCl medium was observed, similar to the weight loss and EIS studies. Linear polarization studies supplemented this observation. From Tafel plots, both cathodic and anodic Tafel slopes change appreciably in the presence of TCE, suggesting that TCE act as a mixed type inhibitor.

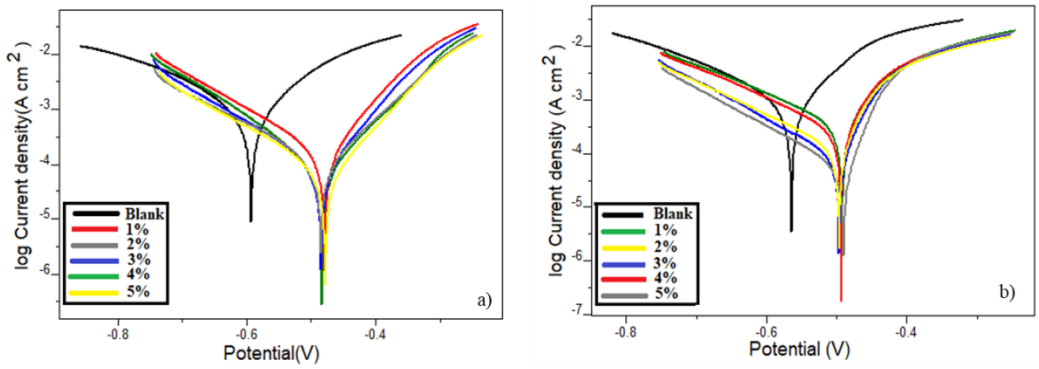

Fig. 5.10: Tafel plots of mild steel with and without TCE in a) 1 M HCl and b) 0.5 M H_2SO_4

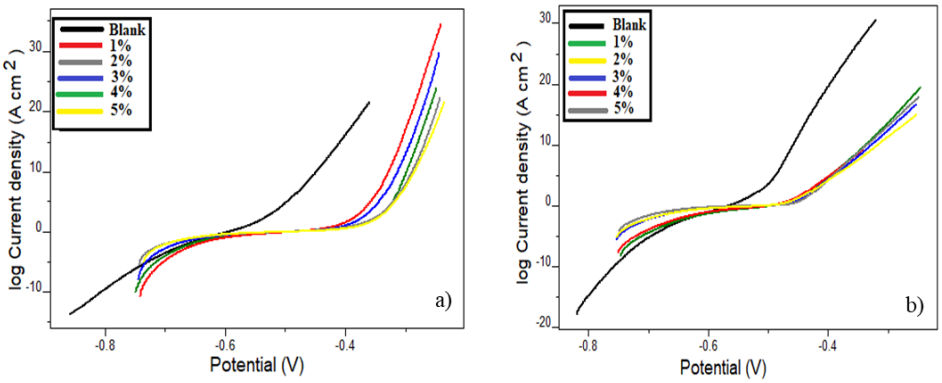

Fig. 5.11: Linear polarization plots of mild steel with and without TCE in a) 1 M HCl and b) 0.5 M H_2SO_4

Table 5.6: Potentiodynamic polarization parameters of mild steel in 1 M HCl and 0.5 M H_2SO_4 with and without TCE

Medium	Conc. (v/v %)	Tafel data					Polarization data	
		$-E_{corr}$ (mV)	i_{corr} ($\mu A/cm^2$)	$-b_c$ (mV/dec)	b_a (mV/dec)	η_{pol}%	R_p (ohm)	η_{Rp}%
1 M HCl	Blank	597.9	1240	221	166	-	33.14	-
	1	489.5	190.9	151	94	84.60	131.9	75.28
	2	486.9	105.1	176	91	91.52	228.9	85.5
	3	473.4	103.5	149	86	91.65	248.5	86.66
	4	472.6	82.12	132	85	93.35	273.9	87.90
	5	468.5	71.62	159	82	94.22	328.4	89.90
0.5 M H_2SO_4	Blank	602.2	1616	193	184	-	25.30	-
	1	562.8	845.2	184	210	46.70	50.35	49.75
	2	595.9	507.1	161	210	67.62	72.14	64.92
	3	599.6	445.1	137	199	71.46	78.24	67.66
	4	529.6	435.6	173	124	72.05	79.14	68.03
	5	609.5	388.0	143	194	75.00	92.12	72.53

Electrochemical noise measurements

Fig. 5.12 reveals the current noise for mild steel dipped in 1 M HCl and 0.5 M H_2SO_4 solutions containing various TCE concentrations (0, 1, 3, 5 v/v %). On inspection of the Figure, it was evident that the current noise for inhibited metal has a low value compared with uninhibited metal, which implies that TCE possesses considerable inhibition efficiency. As concentration increases, the value of current noise becomes lowered. The signal was at a higher magnitude for the blank experiment, indicating mild steel surface undergoes localized corrosion[154].

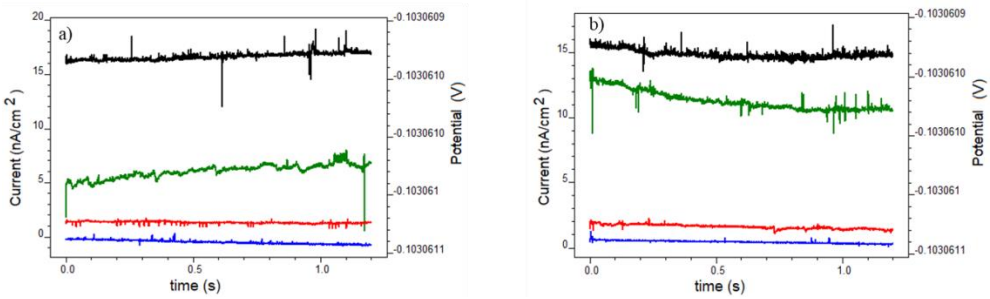

Fig. 5.12: Current noise plots of mild steel with and without TCE in a) 1 M HCl b) 0.5 M H_2SO_4

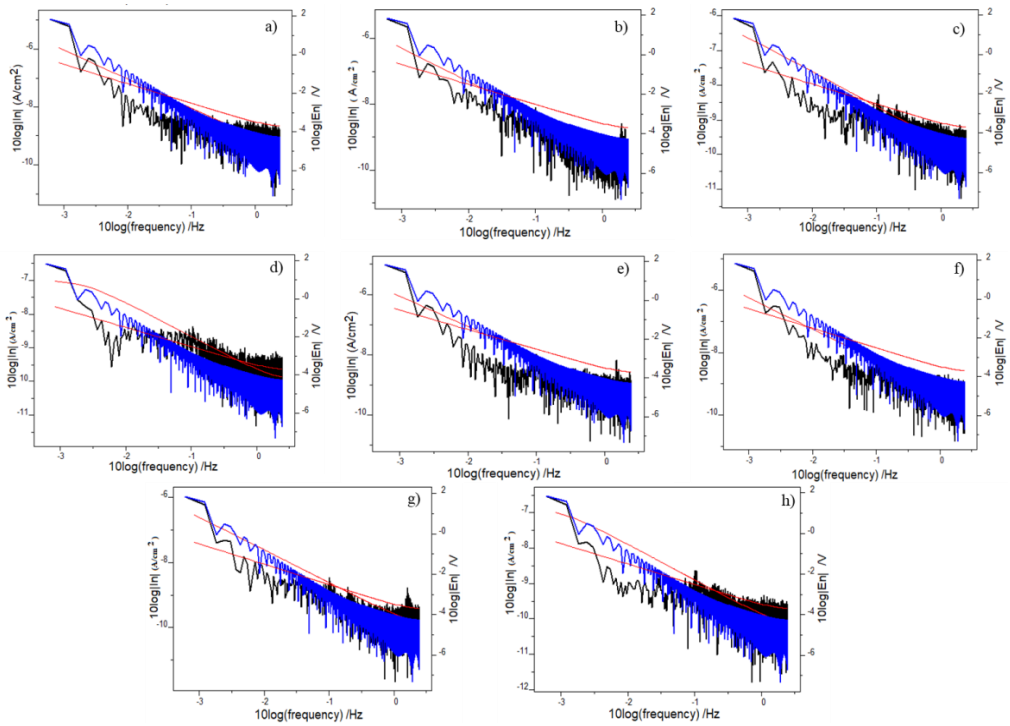

Fig. 5.13: Power spectral density plots of mild steel in 1 M HCl a) without TCE b) 1% TCE c) 3% TCE d) 5% TCE; Power spectral density plots of mild steel in 0.5 M H_2SO_4 e) without TCE f) 1% TCE g) 3% TCE h) 5% TCE

PSD plots for inhibited and uninhibited metal in acid media are shown in Fig. 5.13. It exhibited that magnitudes of current noise are relatively large for metal dipped in acid solution without TCE than the metal immersed in acid solution with TCE, which unequivocally establishing the inhibition action of TCE towards mild steel corrosion.

Pitting index is an assessment of the degree of resistance power to pitting corrosion. Fig. 5.14 shows pitting index curves for mild steel immersed in the absence and presence of various TCE concentrations. It was clear that as the concentration of TCE increases, the pitting index value rises. HCl pitting index value was higher for 5 v/v% concentration, while it was remarkably lower in the H_2SO_4 medium for the same concentration. From the pitting index values for blank and inhibited metal, it can be said that TCE can be acted as an inhibitor for mild steel in acid media[169].

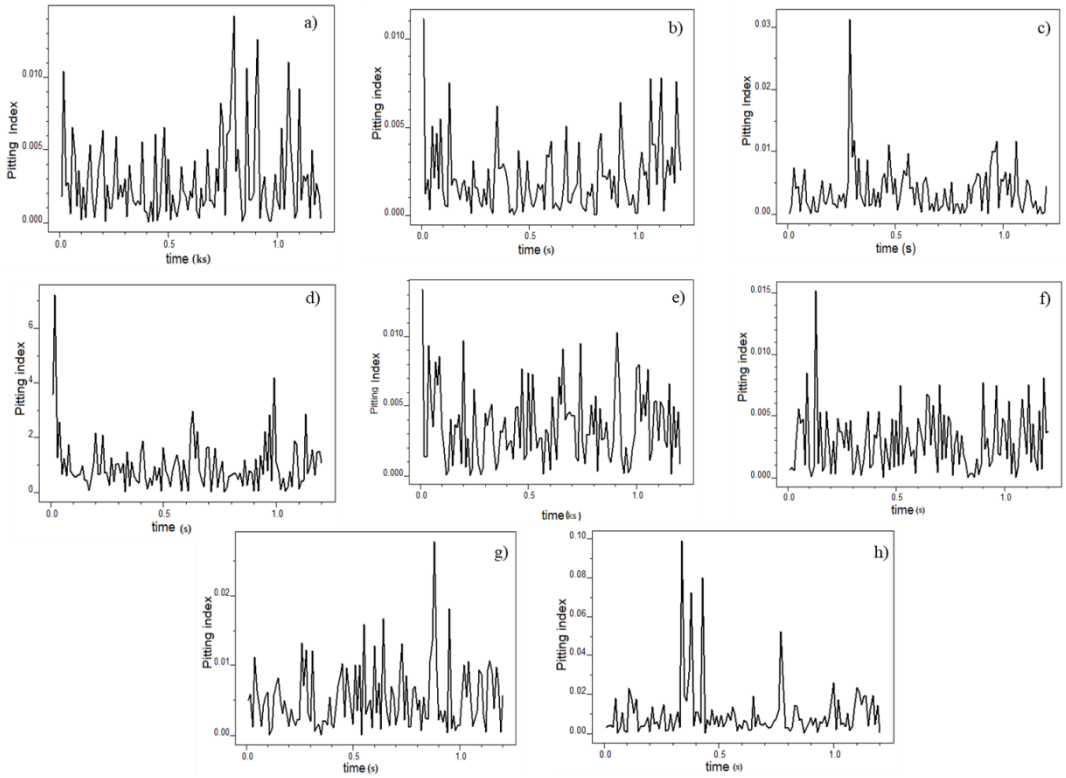

Fig. 5.14: Pitting index curves of mild steel in 1 M HCl a) without TCE b) 1% TCE c) 3% TCE d) 5% TCE; Pitting index curves of mild steel in 0.5 M H_2SO_4 e) without TCE f) 1% TCE g) 3% TCE h) 5% TCE

Atomic force microscopy

Surface mechanism of TCE on mild steel was further strengthened by AFM analysis. 3-D topography of smoothened metal, blank, metal coupons treated with 5 v/v% TCE in 1 M HCl and 0.5 M H_2SO_4 for 24 hrs are exhibit in Fig. 5.15 a–e, respectively. Surface roughness parameters such as average roughness (R_a), root mean square roughness (R_q), and maximum peak-to-peak height (R_{pp}), which specify the topography of surfaces, are provided in Table 5.7.

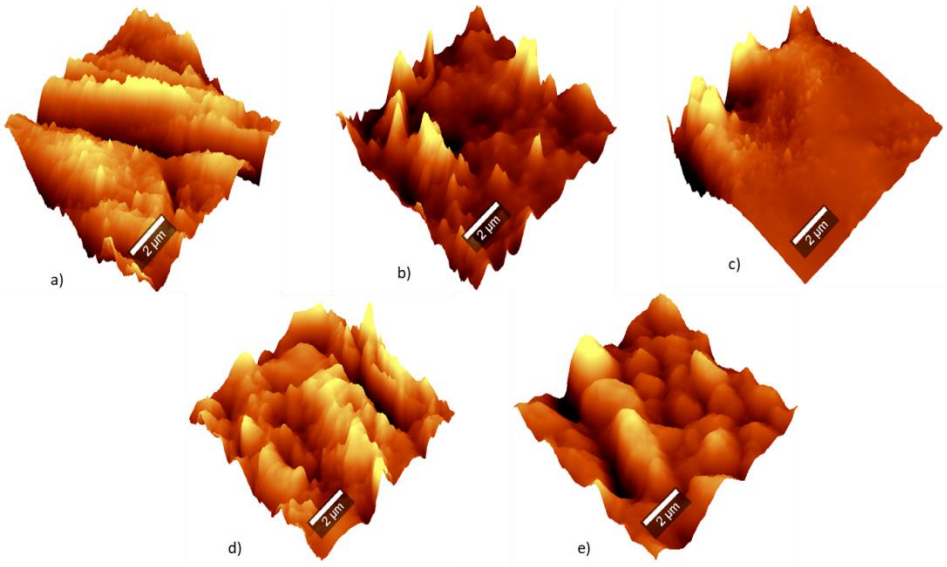

Fig. 5.15: Topography of mild steel surface a) smoothened b) in 1 M HCl c) in 1 M HCl with 5 v/v% TCE d) in 0.5 M H_2SO_4 e) in 0.5 M H_2SO_4 with 5 v/v% TCE

Table 5.7: Surface roughness parameters of mild steel by AFM analysis

Sample	R_{pp} (nm)	R_q (nm)	R_a (nm)
Smoothened mild steel	205.27	32.92	26.11
Mild steel in 1 M HCl	965.86	79.50	55.07
Mild steel in 1 M HCl with 5 v/v% TCE	646.53	51.65	29.57
Mild steel in 0.5 M H_2SO_4	2176.62	231.72	180.48
Mild steel in 0.5 M H_2SO_4 with 5 v/v%	1687.53	177.35	142.65

On analyzing the Table, it can be seen that surface roughness parameters for the smoothened metal were low, whereas the metal treated with 1 M HCl and 0.5 M H_2SO_4

were boosted due to the contact with aggressive media. Roughness parameters of the metal surface with TCE were in between that of smoothened and blank metals. It reinforces the adsorption of inhibitor molecules on the metal surface in the corrosion reaction[60]. It has also been noticed that the roughness parameters for the metal with TCE in 1 M HCl were lower than in 0.5 M H_2SO_4, implying that the former medium supports the mitigation of corrosion than the latter.

Quantum mechanical calculations

Quantum mechanical parameters of tinosponone such as energy values of HOMO and LUMO, ΔE, ionization energy (I), electron affinity (A), chemical potential (μ), electronegativity (χ), chemical hardness (η) and number of electrons transferred (ΔN) are computed in Table 5.8. The optimized geometry, corresponding HOMO and LUMO of tinosponone are pictured in Fig. 5.16. Formation of the adsorption layer on the mild steel surface by the donation of electrons can be demonstrated by the value of change in energy (E_{LUMO} - E_{HOMO}). The low ΔE value (4.178 eV) for tinosponone enables the shifting of electrons from HOMO of tinosponone to the vacant orbitals of Fe and makes TCE an excellent metal protection inhibitor. Value of ΔN less than 3.6 indicates a strong propensity for inhibitor molecules to supply electrons to the metal surface. For tinosponone ΔN value was found to be 1.4265, which may be ascribed to the excellent corrosion control of TCE[160]. So, theoretical calculations were in line with experimental results.

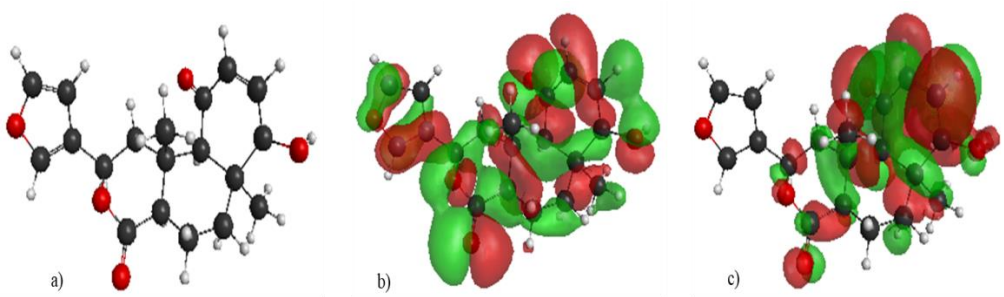

Fig. 5.16: a) Optimized geometry, b) HOMO and c) LUMO of tinosponone

Table 5.8: Quantum mechanical parameters (in eV) of tinosponone

E_{HOMO}	E_{LUMO}	ΔE	I	A	μ	χ	η	ΔN
-3.129	1.049	4.178	3.129	-1.049	-1.04	1.04	2.089	1.4265

Statistical analysis

❖ ***Optimization of factors for inhibition efficiency (IE%)***

Screening experiments revealed that temperature, TCE concentration, and acid concentration significantly influenced the corrosion inhibition efficiency. So they were selected as independent factors in this study. Weight loss studies showed that the corrosion rate was upgraded in H_2SO_4 medium than in HCl medium. That prompted us to select the HCl solution as an acid medium. The structure of the design and the three levels depending on the BBD of test factors are shown in Table 5.9, comprising experimental results and predicted response. A total of 15 experimental runs were obtained in it. It was demonstrated that corrosion inhibition efficiency increased with an increase in TCE concentration. This analysis reached maximum efficiency with 5 v/v% TCE concentration in 0.5 M HCl concentration at 313 K. To explore the exact combination of the three factors understudy for attaining the immense efficiency, RSM was applied for the optimization technique. The regression model between the test factors and the inhibition efficiency was created at that point, shown in equation (53). Inhibitor efficiency was designated as a function of the test factors in the selected levels using the quadratic equation (53).

$$IE = 5891 - 34.44\ X_1 + 30.3X_2 - 264.1\ X_3 + 0.0503\ X_1^2 - 1.387\ X_2^2 - 20.79\ X_3^2 + 0.922\ X_1X_3 - 1.62\ X_2X_3 - 0.0397\ X_1X_2 \quad (53)$$

where IE represents inhibition efficiency, X_1 denotes temperature, X_2 denotes TCE concentration and X_3 denotes acid concentration.

Using this regression model, analysis of variance (ANOVA) was then applied. ANOVA results with a significance level of 95% are illustrated in Table 5.10. The most

demanding parameter is P-value in this Table. P-value determined shows the significance of the impact of a factor on response[170]. The degree of essentialness (α) was chosen to be 0.05. It showed that the value of P was lower than 0.05 for the linear and square terms. The ANOVA results explained that TCE concentration was the factor having a significant influence on the response. Pareto chart (Fig. 5.17) describes that three linear terms such as temperature, TCE concentration and acid concentration have an appreciable impact on the inhibition efficiency in which TCE concentration has the most. Squared terms of temperature, TCE concentration and acid concentration were found to have a low influence on IE%. The two-way interaction term X_1X_3 also exhibited a small impact on IE%, whereas the remaining interaction terms X_1X_2 and X_2X_3 did not reveal any impact on the inhibition efficiency.

Table 5.9: Experimental and predicted IE% from weight loss measurements and BBD

Run order	Actual level of factors			IE%		Residual
	X_1	X_2	X_3	Experimental	Predicted	
1	313	1	1	60.11293	57.7645	2.34843
2	333	1	1	35.54071	36.4269	0.88619
3	313	5	1	90.39050	89.5043	0.88619
4	333	5	1	62.64005	64.9884	2.34835
5	313	3	0.5	84.60215	84.8844	0.28225
6	333	3	0.5	55.68507	52.7327	2.95237
7	313	3	1.5	60.13363	63.0860	2.95237
8	333	3	1.5	49.66637	49.3841	0.28226
9	323	1	0.5	39.46750	41.5337	2.06620
10	323	5	0.5	74.32543	74.9294	0.60397
11	323	1	1.5	32.80916	32.2052	0.60396
12	323	5	1.5	61.17699	59.1108	2.06619
13	323	3	1	62.68992	62.6899	0.00001
14	323	3	1	62.68992	62.6899	0.00001
15	323	3	1	62.68992	62.6899	0.00001

The better fit model for experimental results is indicated by the closeness of R^2 and R^2(adj) value to unity. Here, the R^2 and R^2(adj) values were 0.9892 and 0.9697,

respectively indicate the best fit predicted model for experimental values. Therefore, the outcomes can be quickly evaluated by the model.

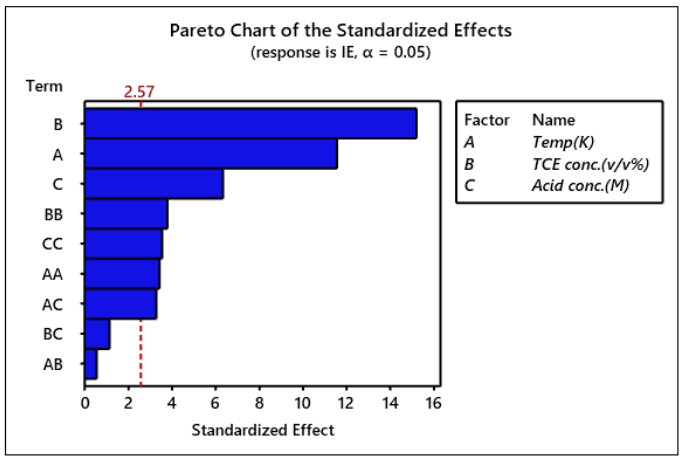

Fig. 5.17: Pareto chart of the standardized effects of mild steel

Table 5.10: Analysis of variance for corrosion inhibition efficiency

Source	DF	Adj SS	Adj MS	F-Value	P-Value
Model	9	3607.35	400.82	50.79	0.000
Linear	3	3185.58	1061.86	134.55	0.000
Temp	1	1051.27	1051.27	133.21	0.000
TCE Conc.	1	1818.13	1818.13	230.37	0.000
Acid Conc.	1	316.19	316.19	40.06	0.001
Square	3	323.62	107.87	13.67	0.008
Temp*Temp	1	93.38	93.38	11.83	0.018
TCE Conc.*TCE Conc.	1	113.65	113.65	14.40	0.013
Acid Conc.*Acid Conc.	1	99.73	99.73	12.64	0.016
2-Way Interaction	3	98.15	32.72	4.15	0.080
Temp*TCE Conc.	1	2.53	2.53	0.32	0.596
Temp*Acid Conc.	1	85.10	85.10	10.78	0.022
TCE Conc.*Acid Conc.	1	10.53	10.53	1.33	0.300
Error	5	39.46	7.89		
Lack-of-Fit	3	39.46	13.15	*	*
Pure Error	2	0.00	0.00		
Total	14	3646.81			

DF: degrees of freedom, Adj SS: adjusted sum of squares, Adj MS: adjusted mean of squares,

F: Fischer's F-test value, P: probability

Main effects plots supplement the outcomes obtained from the regression analysis[171]. It represents how to control tested factors that influence the response. Fig. 5.18 explains the main effects plots for the fitted means of inhibition efficiency. It

showed that the maximum inhibition efficiency was observed for 5 v/v% concentration of TCE at an operating temperature of 313 K at 0.5 M concentration of HCl. Rise in temperature causes a hike in the kinetic energy of the inhibitor molecules and the speed of collision between the molecules. This inclination hinders and destroys the development of adsorbed film inhibitors on the metal surface. So, when the temperature goes up, inhibition efficiency decreases. A close tendency was examined with the concentration of HCl as it was raised from 0.5 M to 1.5 M. Whereas inhibition power of TCE augmented when its concentration was increased from 1 to 5 v/v%. The corrosion rate was much boosted in the absence of an inhibitor and reduced when the inhibitor was present. Thereby adsorption of inhibitor molecules enhances, and efficiency also increases.

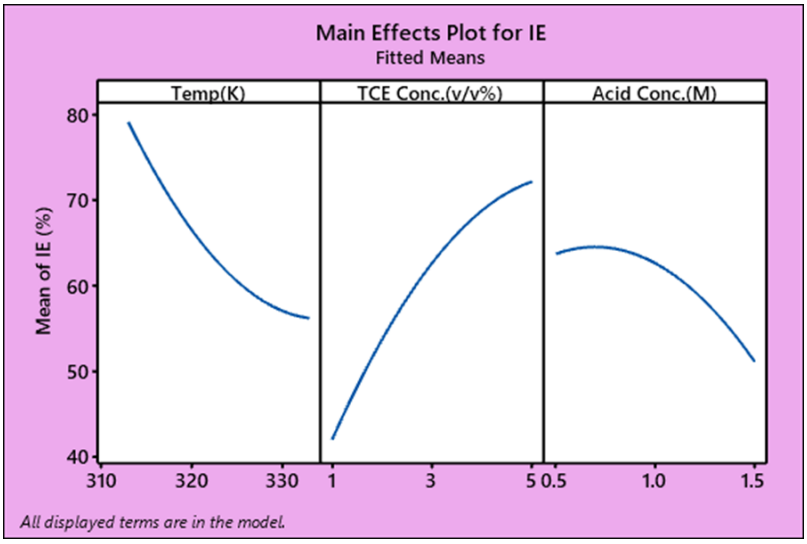

Fig. 5.18: Main effects plots for inhibition efficiency of mild steel in HCl medium

If the change in response is disparate for two factors, there will be an interaction between them. Fig. 5.19 exhibits the interaction plot for inhibition efficiency. Crossed lines in the interaction plot indicate a significant interaction between the factors, whereas parallel or straight lines point out little interaction[134]. From Fig. 5.19, it has been examined that the two-way interaction terms were trivial as there are no crossed lines except in Temp-Acid concentration interaction term, X_1X_3. Outcomes of ANOVA

analysis also revealed that the P-value was higher than 0.05 for two-way interactions, and only one interaction term has a lower P-value, i.e., X_1X_3.

Contours and 3-D surface plots demonstrate the inter-dependence of the tested factors on IE (%) and are presented in Fig. 5.20. It was exhibited that the inhibition efficiency goes up when TCE concentration rises for a given temperature. But, inhibition efficiency and temperature have a reverse relationship. This trend can be ascribed to the physical adsorption of TCE molecules on the mild steel surface. Similarly, inhibition efficiency and acid concentration are inversely proportional.

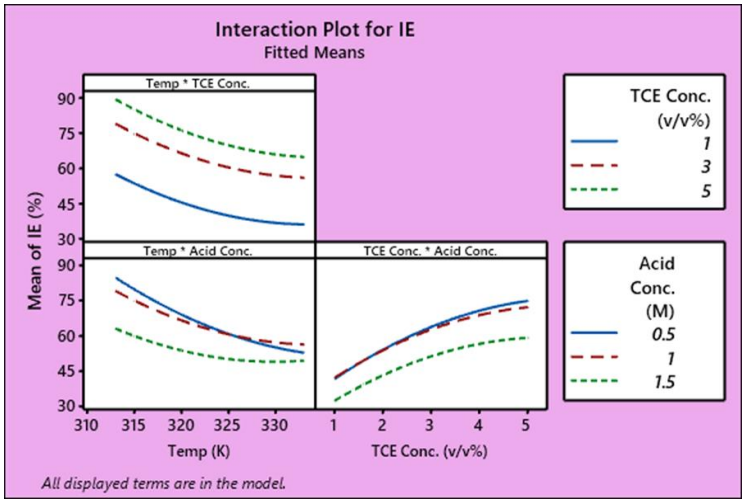

Fig. 5.19: Interaction plot for inhibition efficiency

❖ ***Response optimization***

Well organized numerical model in equation (53) was used with the goal of optimizing the independent variables such as temperature, TCE concentration and acid concentration to bring about the maximum IE. For the most remarkable and feasible response, the desirability function method was employed by improving tested factors[172]. Response optimization plot for IE is shown in Fig. 5.21. The anticipated optimum factors identified were temperature (313 K), TCE concentration (5 v/v%), and acid concentration (0.5 M) for the HCl environment and the corresponding predicted IE was 96.82%, as depicted in Fig. 5.21. Confirmation tests achieved validation of the optimal factor settings and the amelioration of the IE. Confirmation tests were also helped to

verify the recurrence of the experimental outcomes and approve the prescient model's accuracy.

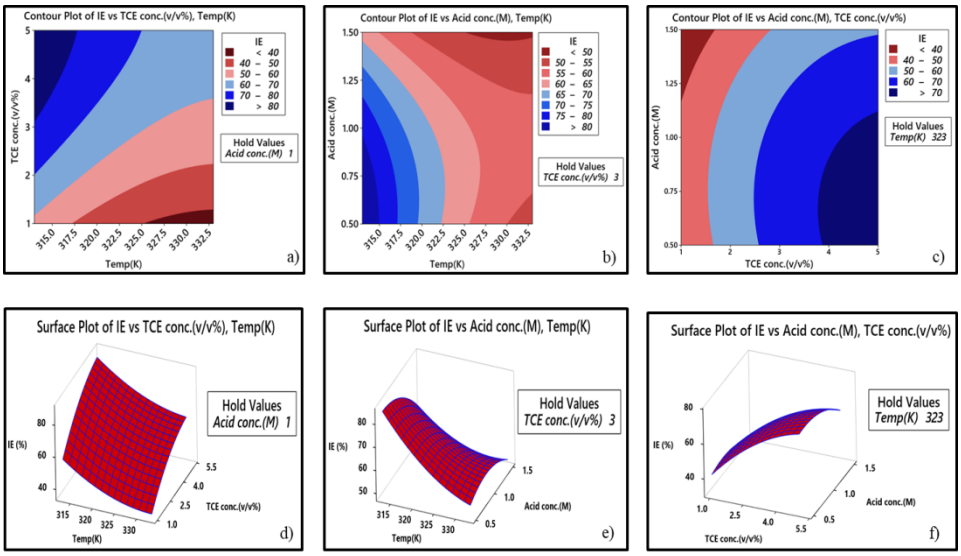

Fig. 5.20: a, b & c) Contours and d, e & f) 3-D surface plots for inhibition efficiency

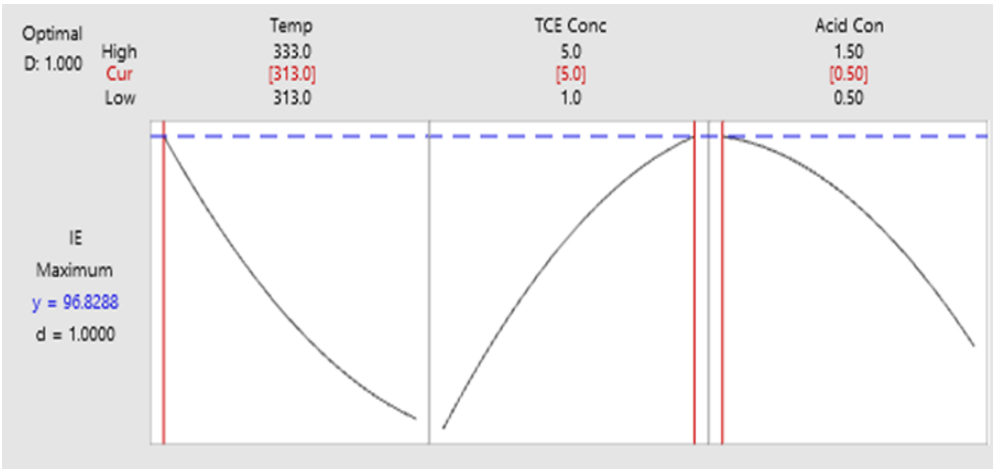

Fig. 5.21: Response optimization plot for inhibition efficiency

Conclusions

- TCE inhibitor was found to diminish and retard the corrosion of mild steel exposed in 1 M HCl and 0.5 M H_2SO_4.
- Weight loss studies showed that boosting the TCE concentration causes an increase in inhibition efficiency due to the adsorption of TCE molecules on the metal surface.

- In comparison, an increment in temperature reduces its inhibition potential due to the desorption of the adsorbed layer.
- Maximum inhibition potency of TCE in 1 M HCl and 0.5 M H_2SO_4 was calculated as 94.73% and 82.53%, respectively.
- Langmuir adsorption isotherm was reckoned to be good adsorption of TCE molecules on mild steel surface in both acid media.
- The variation in surface morphology of mild steel was studied by AFM, which furnished strong proof for developing a protective film on mild steel with TCE in an acidic media.
- Quantum chemical investigations were also supported to confirm the inhibition efficiency of TCE.
- Response surface methodology provides comprehensive information about the interrelation between the factors and the acceptance of the optimum parameter setting. Regression model could describe the results obtained from experiments in good agreement.